Journal of Organometallic Chemistry, 478 (1994) 179–188

Mono-, di- and tri-metallic complexes of trimethylenemethane: an EHMO study of the TMM rotational barrier

Luc Girard [a,b], Michael C. Baird [a], Michael J. Chetcuti [c] and Michael J. McGlinchey [b]

[a] *Department of Chemistry, Queen's University, Kingston, Ont., K7L 3N6 (Canada)*
[b] *Department of Chemistry, McMaster University, Hamilton, Ont., L8S 4M1 (Canada)*
[c] *Department of Chemistry and Biochemistry, University of Notre Dame, Notre Dame, IN 46556 (USA)*

Received October 6, 1993; revised manuscript received December 17, 1993

Abstract

The rotational barrier of a trimethylenemethane ligand relative to an $Fe(CO)_2L$ unit, where L = CO or a phosphine, is analyzed by molecular orbital calculations at the extended Hückel level. It is shown that the original Hoffmann-Albright model fits well for carbonyl complexes, but yields barriers for phosphine complexes that are too high. A rationale is presented to account for the different behavior of the bimetallic complexes $Cp_2M'M''(CO)_2(TMM)$, where M' = M'' = Ru, **2**, (trimethylenemethane (TMM) non-fluxional), and for M' = W and M'' = Ni, **3**, where the TMM rotates. Finally, calculations reveal that the trimetallic complex $[(TMM)Co_3(CO)_9]^+$ should be a stable and non-fluxional system with an eclipsed conformation.

Key words: Iron; Ruthenium; Tungsten; Nickel; Trimethylenemethane; EHMO calculations

1. Introduction

Trimethylenemethane (TMM) is a short-lived species which can be stabilized by a number of ML_n fragments. These are typified by the iron carbonyl complex, $(\eta^4$-TMM)$Fe(CO)_3$, in which the three-fold symmetry of the ligand is maintained. The ground state structure has been established as the staggered isomer, **1a**, in which the iron may be regarded as being in a pseudo-octahedral environment [1]. This high symmetry precludes direct measurement of the barrier to TMM rotation about the three-fold axis; hence, one must resort to a calculational approach to evaluate the energy difference between **1a** and the corresponding eclipsed rotamer **1b**. Experimentally, it is necessary to lower the molecular symmetry either by modifying the TMM moiety itself, or by replacing a carbonyl group on iron by a different ligand.

In the course of their pioneering investigations on the molecular dynamics of organometallic systems, Hoffmann and Albright [2] have probed the electronic barrier to TMM rotation in **1** by means of molecular orbital calculations at the extended Hückel level. In these computations, the effect on the barrier of changing the ligands bonded to the iron center was also examined. Initially, a planar geometry was assumed for the $C(CH_2)_3$ fragment, but it was subsequently modified to take account of the pyramidal nature of the trimethylenemethane moiety in $(TMM)Fe(CO)_3$. The conclusions drawn were that replacement of the carbon monoxide ligands in **1** by PH_3 substituents should lead to a significant increase in the rotational barrier. However, recent experimental data [4,5] on a series of $(TMM)Fe(CO)_2L$ complexes, where L = PMe_3, PMe_2Ph, $AsPh_3$, etc., are not in accord with these predictions and we here describe our own attempts to resolve these apparently conflicting results.

TMM has been shown to be capable of binding not only to monometallic units but also to dimetallic fragments, as in $Cp_2M'M''(CO)_2(TMM)$, where M' = M'' = Ru, **2**, [6] or M' = W and M'' = Ni, **3**, [7]. In the homo-dimetallic system $(C_5H_5)_2Ru_2(CO)_2(TMM)$, **2**, there is no evidence for TMM rotation relative to the Ru–Ru vector, even at elevated temperatures; in contrast, in the hetero-dimetallic complex $(C_5H_5)W(\mu$-

Correspondence to: Prof. M.J. McGlinchey.

0022-328X/94/$7.00
SSDI 0022-328X(94)24437-N

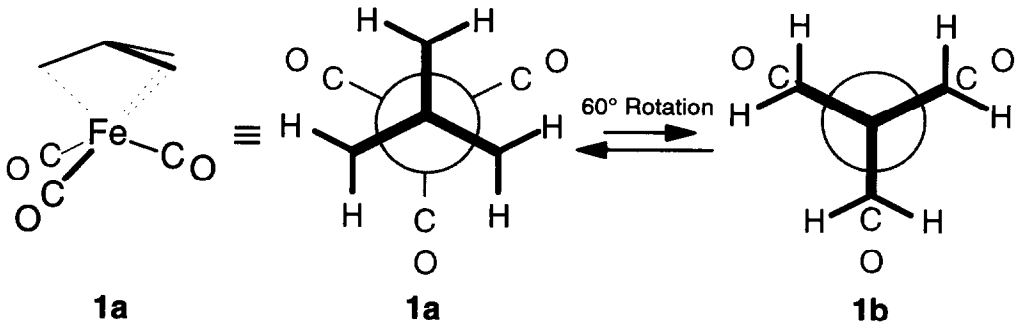

1a 1a 1b

$CO)_2Ni(C_5Me_5)$(TMM), **3**, the TMM is observed to rotate relative to the Ni–W bond with a barrier, $\Delta G^{\ddagger}$, of approximately 15.5 kcal mol^{-1}. Again, we describe the use of EHMO calculations to rationalize the different behavior of these isoelectronic (and essentially isostructural) molecules.

Finally, we speculate on the possible existence of a TMM complex based on a trimetallic framework, and offer some predictions concerning its molecular dynamics.

2. Results and discussion

2.1. Monometallic η^4-TMM complexes

As mentioned above, Hoffmann and Albright [2,3] have investigated the barrier to interconversion of the staggered and eclipsed rotamers of $(\eta^4$-TMM)$Fe(CO)_3$, **1a** and **1b**, respectively. Initial calculations on an assumed planar TMM fragment yielded a rotational barrier of 20.8 kcal mol^{-1} but, when the experimentally established non-planarity of η^4-coordinated TMM was factored in the computed barrier increased to 23.6 kcal mol^{-1} [2]. The bending of the three methylene arms of the ligand towards the iron atom can be rationalized in terms of increased overlap of the TMM donor orbitals with the vacant frontier orbitals of the $Fe(CO)_3$ fragment. Furthermore, if the methylene hydrogens in TMM are allowed to bend away from the iron, the donor orbitals are better hybridized towards the metal. Although the three-fold symmetry precludes direct measurement of the rotational barrier in **1**, such data are available for the molecules **4** and **5**. These monosubstituted complexes yield $\Delta G^{\ddagger}$ values of approximately 17 kcal mol^{-1} and 18 kcal mol^{-1}, respectively [8]. These results are in reasonable accord with the predicted value of ≈ 21 kcal mol^{-1}, and they also show that even the presence of a CH_3-C=O group, which is potentially capable of conjugation with the delocalized TMM system, has little effect on the rotational barrier.

The realization that the TMM ligand in (TMM)$Fe(CO)_3$ is non-planar in the structurally characterized

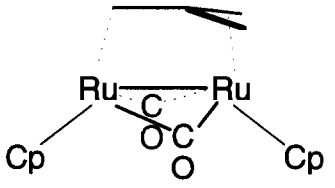

2

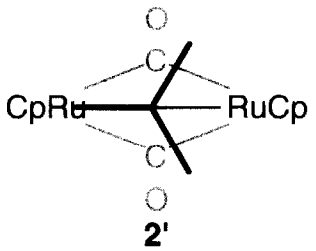

2'

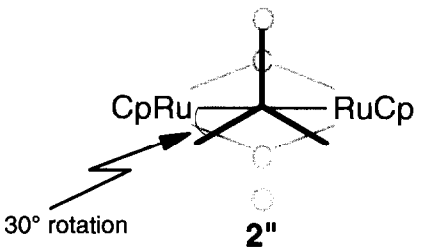

2''

staggered rotamer **1a** raises the question of the geometry of the TMM ligand as it rotates about the three-fold axis of the molecule. Spectroscopically derived force fields for (η^4-TMM)Fe(CO)$_3$ have been reported by several authors [9–11], and these studies have revealed that distortions of the TMM ligand are energetically undemanding relative to those of the carbonyls in the same molecule. The stretching force constants in the TMM moiety are of the order 3–4 mdyn Å^{-1}, significantly less than the 16–17 mdyn Å^{-1} values obtained for the Fe(CO)$_3$ fragment. Thus, we have generated a three-dimensional plot (Fig. 1) which correlates on one axis the TMM group's rotation (relative to the Fe(CO)$_3$ tripod), as well as the deviation from planarity of the TMM (as evidenced by the Fe–C$_{central}$–CH$_2$ angle, ϕ) on a second axis *vs.* the EHMO-computed total energy. It is apparent from Fig. 1 that the barrier to TMM rotation is strongly dependent on the bend angle, ϕ. As anticipated, the global minimum energy is found at the TMM rotation angle of 0° or 120°, and for this rotamer ϕ is favored at 82.5°; the experimental value of ϕ from electron diffraction data is 78° [1]. As the TMM rotates through an angle of 60° (giving the eclipsed structure **1b**) it passes over the saddle point where ϕ is minimized at 85°. That is, rotation of the TMM fragment relative to the Fe(CO)$_3$ tripod is accompanied by a gentle umbrella motion of the three methylene arms of the organic ligand.

To probe the effect of different substituents at the metal center, Hoffmann and coworkers [2] then investigated other molecules of C_{3v} symmetry, *e.g.* (TMM)Fe(PH$_3$)$_3$, **6**, and concluded that the rotational barrier of this hypothetical compound should be significantly higher (32.5 kcal mol^{-1}) than for the parent tricarbonyl, **1**. At that time, experimental evidence was limited to the series (TMM)Fe(PF$_3$)$_n$(CO)$_{3-n}$, described by Clark *et al.* [12]. These compounds, for which the apparent barrier to rotation did increase somewhat with the number of phosphines bound to iron, were not significantly different electronically from (TMM)Fe(CO)$_3$; indeed, the π-acceptor ability of PF$_3$ is well-known to resemble that of carbon monoxide.

Perhaps the closest available analogue of (TMM)Fe(PH$_3$)$_3$, **6**, is the trimethylphosphine complex, (TMM)Fe(PMe$_3$)$_3$, **7**, originally reported by Dixneuf and coworkers [13]. Recent investigations of the chemical reactivity of **7** reveal that the TMM is rather weakly bound and the presence of a large barrier to rotation seems improbable. Typically, attempted [3 + 2] cycloadditions on (TMM)Fe(PMe$_3$)$_3$, **7**, yield instead dimers and higher oligomers of TMM [14]. This contrasts with the behavior of the TMM–palladium sys-

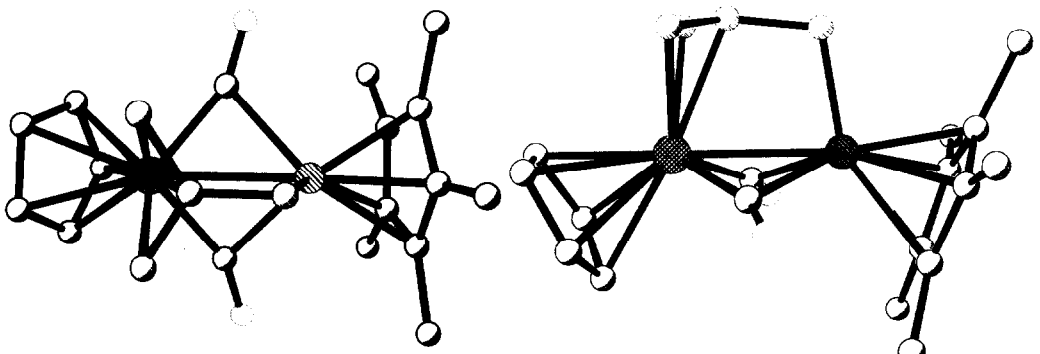

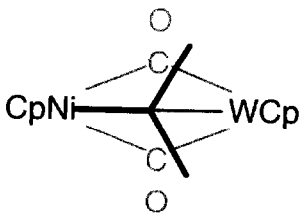

3'

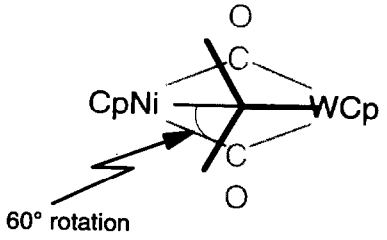

3"

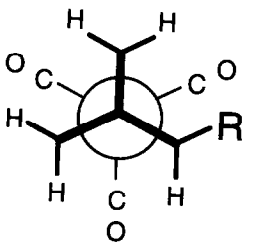

4: R = $CH(OH)CH_3$
5: R = $C(=O)CH_3$

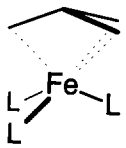

6: L = PH_3
7: L = PMe_3

tems which are well-known to undergo cycloadditions [15]. Subsequently, the more robust species $(TMM)Fe(CO)_2L$, where $L = R_3P$, $AsPh_3$, were synthesized and subjected to detailed variable-temperature NMR studies which revealed that the $\Delta G^{\ddagger}$ values again lay in the range 14.5–18 kcal mol^{-1} [5]. The failure to observe markedly increased rotational barriers for phosphine-substituted trimethylenemethane complexes of iron caused us to reexamine the EHMO-derived predictions.

We note that the original calculations carried out to probe the effect of incorporating phosphine ligands, as in **6**, used a basis set made up of only s and p functions on phosphorus. Normally, such a basis set suffices to describe the behavior of phosphorus in organometallic systems but, occasionally, it has been found advantageous to expand the basis set to include d orbitals; for example, Vahrenkamp's octahedral clusters such as $[Fe(CO)_3]_4(PR)_2$ possess eight, rather than seven, skeletal electron pairs [16]. The addition of d orbitals to the phosphorus atoms allows the extra pair of electrons to reside in a more strongly bonding orbital of δ symmetry [17]. Of course, the question of basis sets has long been a contentious topic; for example, numerous authors have chosen to rationalize the planarity of trisilylamine, $N(SiH_3)_3$, or the large Si–O–Si angles in silyl ethers, in terms of $p\pi$–$d\pi$ interactions [18]. We have no wish to become embroiled in such controver-

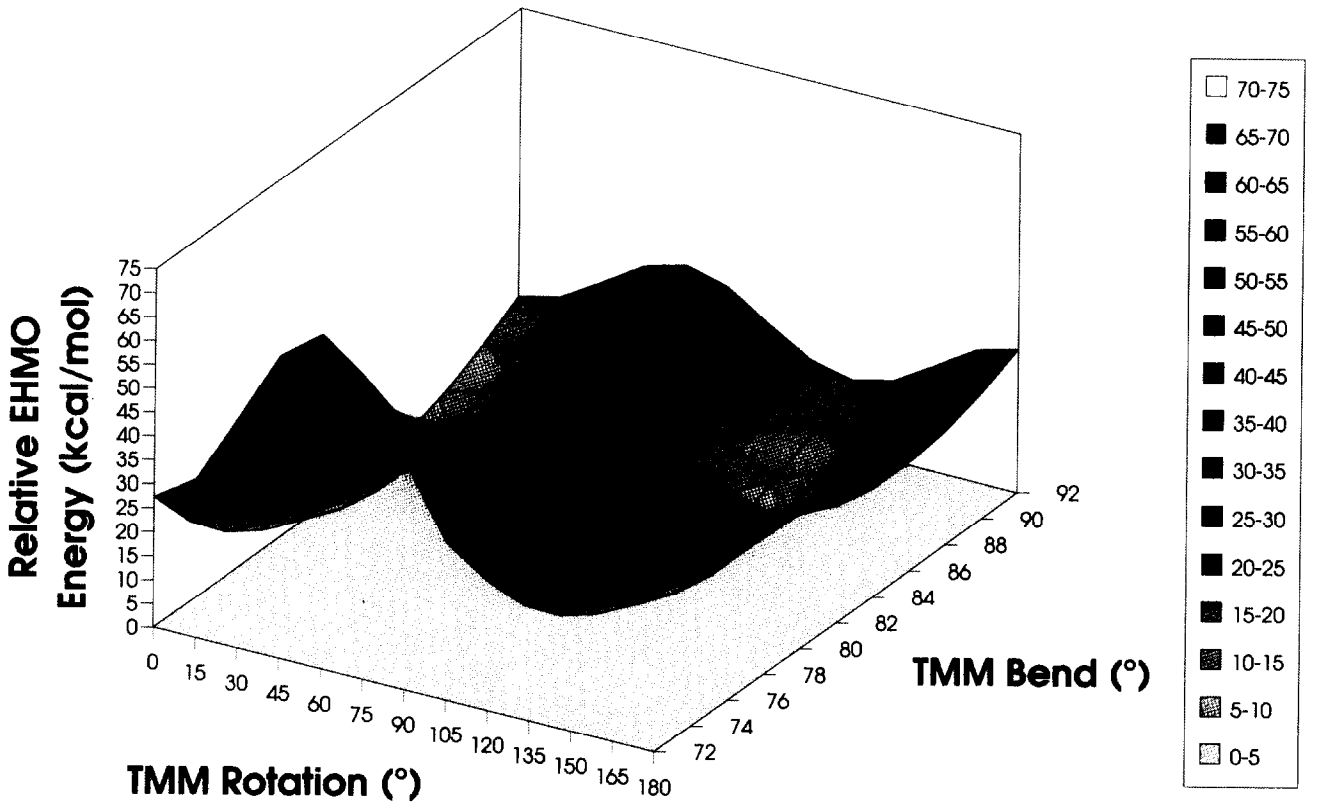

Fig. 1. Energy hypersurface for the concomitant bending and rotation of the TMM ligand in $(\eta^4$-TMM)$Fe(CO)_3$, **1**.

sies and make no comment on the bonding in those fascinating molecules, but we do note that use of a basis set including phosphorus d orbitals yields an EHMO-derived barrier of 11 kcal mol^{-1} for (TMM)-$Fe(PMe_3)_3$, **7**. However, the majority of recent commentators [19] have rejected the use of d orbitals to rationalize the bonding in Si–O–Si systems, or in metal–phosphine complexes. Nevertheless, it would seem that it is necessary to provide a mechanism for the phosphine ligands to accept some electron density from the metal and not merely function as σ-donors. As Orpen has noted, the traditional model of π back-bonding in metal–phosphine complexes invokes purely 3d acceptor orbitals on phosphorus but, in systems of the type L_nM-PA_3, the involvement of orbitals of P-A σ^* character is becoming increasingly accepted [19f].

In light of these EHMO studies of the electronic barriers towards the rotation of TMM relative to phosphine-containing tripods, we attempted to describe the steric impact of the phosphines on the TMM rotation barrier. To this end, the program PC-MODEL [20,21] was used to generate a 3D surface where the TMM ligand rotates simultaneously with the Fe–P bond in the compound (η^4-TMM)$Fe(CO)_2PPh_3$. As the maximum barrier in this 3D surface was found to be ≈ 5 kcal mol^{-1}, significantly less than the experimental barriers, one is drawn to the conclusion that steric effects are not the major components of the rotational barriers.

We have carried out preliminary calculations on the relative rotational barriers in species such as (η^4-diene)$Fe(CO)_3$ and (η^4-diene)$Fe(CO)_2PR_3$; again, use of a phosphorus basis set including only s and p functions predicts a sizeable increase in the barrier for the phosphine-substituted complex. However, the available experimental data yield markedly reduced $\Delta G^{\ddagger}$ values relative to those observed for the parent tricarbonyls [22]. Clearly, this area merits further study.

2.2. *Bimetallic η^4-TMM complexes*

The rotation of TMM relative to a dinuclear fragment can be envisaged for both the homo-bimetallic and hetero-bimetallic cases. The former is represented by Knox and coworkers $(C_5H_5)_2Ru_2(CO)_2$(TMM), **2**, which does not exhibit TMM rotation [6], and the latter by Chetcuti *et al.*, $(C_5H_5)W(\mu\text{-}CO)_2Ni(C_5Me_5)$-(TMM), **3**, which is fluxional [7]. The X-ray crystal structure of **2** yields the asymmetric geometry **8** but, at higher temperatures, there is compelling IR and NMR evidence [6] for the formation of the C_s isomer **2'**; it is this latter molecule which we now discuss. The two fragments $(CpRu(\mu\text{-}CO)_2RuCp]^{2+}$ and $[TMM]^{2-}$ have C_{2v} and C_{3v} symmetry, respectively. These moieties

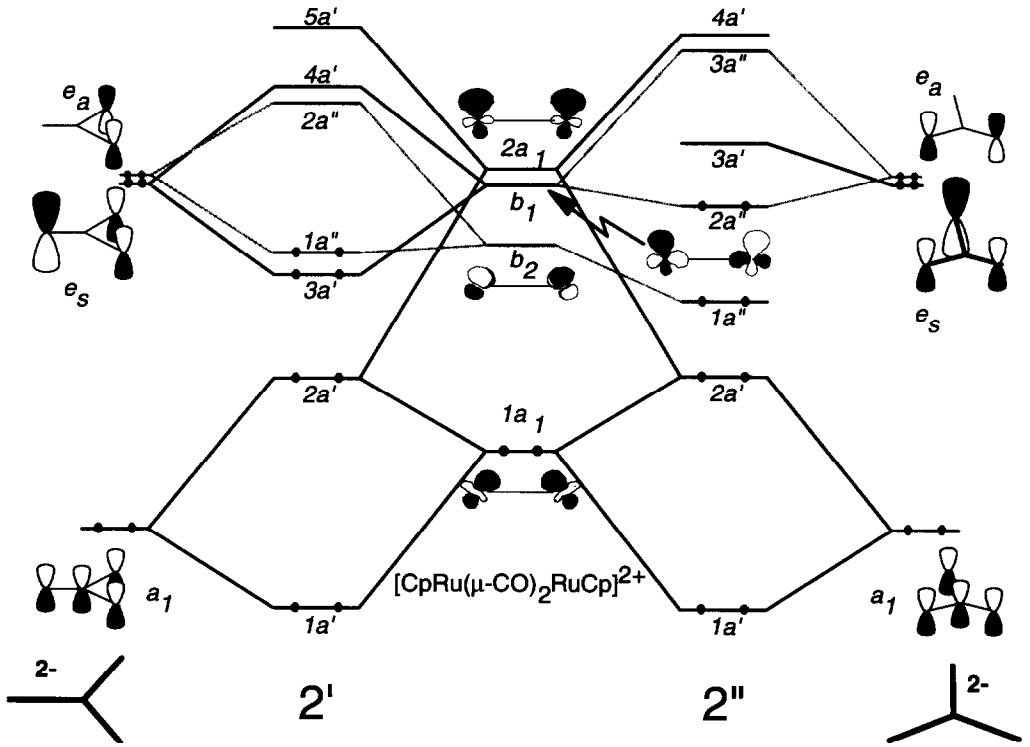

Fig. 2. Frontier orbital interaction diagram for the parallel and transverse rotamers of $(C_5H_5)_2Ru_2(CO)_2$(TMM), **2'** and **2"**.

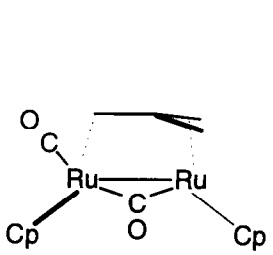

8

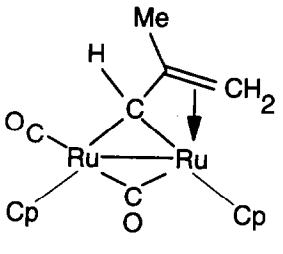

9

possess a single mirror plane in common: in the ground state structure **2'** the *xz* mirror contains the two ruthenium but, in rotamer **2''**, the metal atoms straddle the *yz* symmetry plane.

The non-planar $[TMM]^{2-}$ ligand possesses three filled π-type orbitals, *viz.* the totally symmetric a_1 combination, and a higher-lying e pair (designated e_s and e_a in the C_s point group). Note that rotation of the TMM ligand through 30° generates isomer **2''** in which the molecular mirror plane has turned through 90°. The frontier orbitals of the C_{2v} $(CpRu(\mu\text{-}CO)_2RuCp]^{2+}$ fragment are shown in Fig. 2. The three lowest-lying vacant orbitals are of appropriate symmetry and energy to interact with the π-donor orbitals of the trimethylenemethane dianion. The LUMO of the $[CpRu(\mu\text{-}CO)_2RuCp]^{2+}$ fragment has δ^* character and is made up of an out-of-phase combination of metal d_{yz} orbitals. This b_2 orbital is antisymmetric in both the parallel, **2'**, and transverse, **2''**, isomers. In contrast, the vacant b_1 orbital is symmetrical in **2'** but antisymmetric in **2''**. The other two orbitals of interest are the filled $1a_1$ and vacant $2a_1$ levels, both of which are symmetrical whether the TMM ligand is aligned parallel, **2'**, or perpendicular, **2''**, to the Ru–Ru axis.

As depicted in Fig. 2, the filled $1a_1$ and vacant $2a_1$ metal combinations mix with the low-lying totally symmetric TMM a_1 orbital giving rise to a three-orbital, four-electron set which is unaffected by TMM rotation. In this respect, the dinuclear complexes are analogous to the monometallic systems, where the orientation of the TMM ligand is controlled by the interactions of the e_s and e_a donor orbitals with the acceptor orbitals on the metal fragment. In the ground state orientation, **2'**, the Ru_2 b_1 combination is not only symmetric but is also ideally oriented for overlap with the e_s component of the $[TMM]^{2-}$ HOMO. Concomitantly, the TMM e_a orbital finds a symmetry match with the vacant metal $b_2(\delta^*)$ combination; however, the overlap is noticeably less than is found for their symmetrical (b_1) counterparts, and it is the antisymmetric (b_2) orbitals which have a smaller splitting and give rise to the HOMO and LUMO in **2'**.

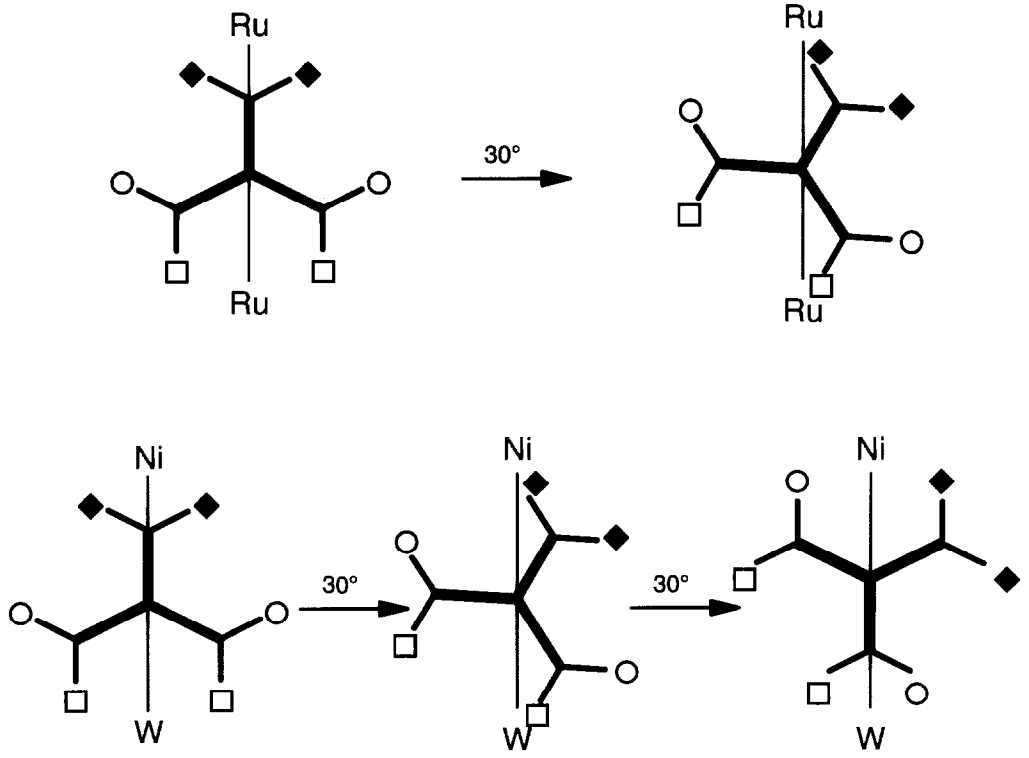

Fig. 3. Labelled rotamers showing that in **2**, the protons are equilibrated by a 30° rotation; in **3**, a 60° rotation is required.

When the TMM adopts the transverse orientation, **2''**, it is the TMM e_a component which interacts with the Ru_2 b_1 combination (which is now antisymmetric with respect to the molecular mirror plane that bisects the metal–metal bond). The crucial factor, which destabilizes **2''** relative to **2'**, is the absence of a suitable symmetric orbital on the dimetallic fragment which could accept electron density from the e_s component of the HOMO in $[TMM]^{2-}$. As is clear from Fig. 2, the net result is a greatly reduced HOMO–LUMO gap (1.38 eV in **2'**; 0.53 eV in **2''**) which, together with the overall less favorable total energy, strongly disfavors the TMM rotation required to interconvert the parallel structure **2'** and the transverse rotamer **2''**. Indeed, the Walsh diagram for this transformation reveals that the orbital composed of the Ru_2 b_1 combination with the e_s component from $[TMM]^{2-}$, which is strongly bonding and occupied in **2'**, correlates with the LUMO in **2''**, and the process is symmetry forbidden. Indeed, Knox has found that **2**, when heated, isomerizes to give the μ-allylidene complex **9**, and the mechanism appears to involve metal–metal bond cleavage [6].

Before discussing the molecular orbital picture of the hetero-bimetallic complex **3'**, we note that equilibration of the three proton environments in $(C_5H_5)_2Ru_2(CO)_2(TMM)$, **2**, requires only a 30° rotation, as shown in Fig. 3. This is not the case for **3'**, and the three TMM ^1H environments (or the 2:1 ^{13}C resonances) are only interchanged when the TMM has executed a 60° rotation, as in **3''**. This not only regenerates the molecular mirror plane containing the metal–metal bond but also renders the trimethylenemethane η^3-bonded to nickel and η^1-linked to tungsten. It is these two C_s isomers, **3'** and **3''**, which we now examine.

The frontier orbitals of the $[CpW(\mu\text{-}CO)_2NiCp]^{2+}$ fragment, while superficially similar to those of the diruthenium unit previously described, differ in one very important aspect, *i.e.* the vacant low-lying acceptor orbitals are heavily localized on tungsten. This is typified by the vacant δ^* orbital made up of an out-of-phase combination of tungsten and nickel d_{yz} orbitals. In the LUMO of $(CpRu(\mu\text{-}CO)_2RuCp]^{2+}$, each metal d_{yz} contributes equally to the orbital; in $[CpW(\mu\text{-}CO)_2NiCp]^{2+}$, this δ^* combination has 54% tungsten character and only a 2% contribution from nickel. Thus, as shown in Fig. 4, overlap of the filled e_a component from $[TMM]^{2-}$ to this vacant δ^* acceptor on $[CpW(\mu\text{-}CO)_2NiCp]^{2+}$ is excellent in **3'**, but rather poor in **3''** where the d_{yz} coefficient on nickel is small. Indeed, in the X-ray crystal structure of **3**, the TMM is not positioned with the central carbon above the mid-

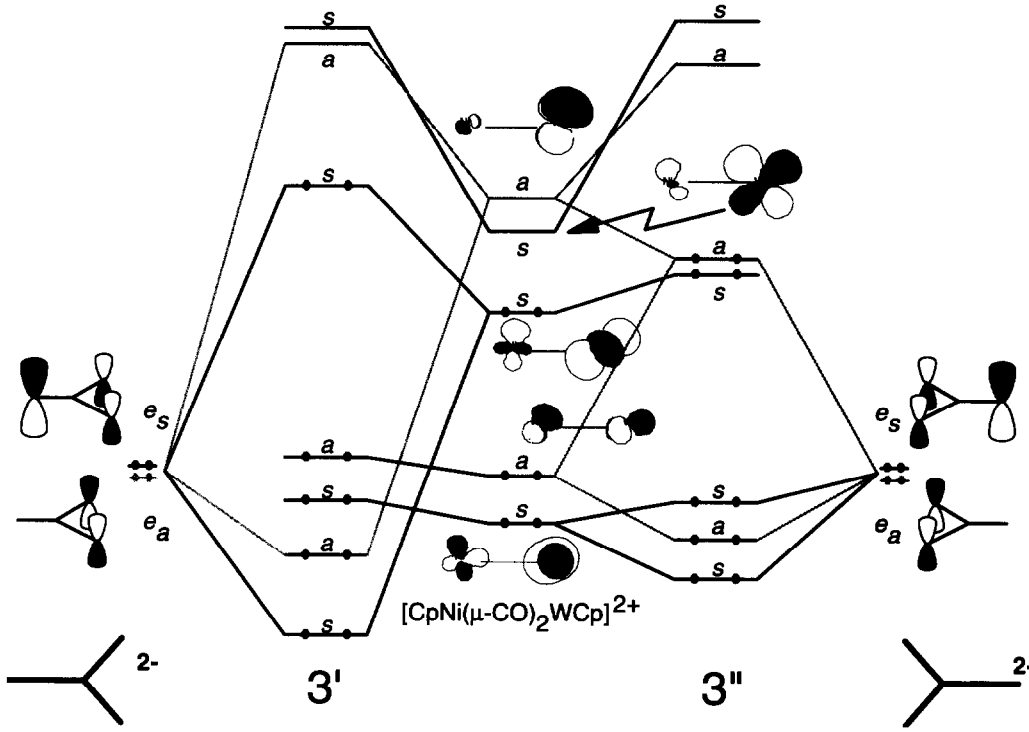

Fig. 4. Frontier orbital interaction diagram for the parallel rotamers of $[CpW(\mu\text{-}CO)_2NiCp][(\eta^3\text{-}W)\text{-}TMM]$, **3'**, and $[CpW(\mu\text{-}CO)_2NiCp][(\eta^3\text{-}Ni)\text{-}TMM]$, **3''**.

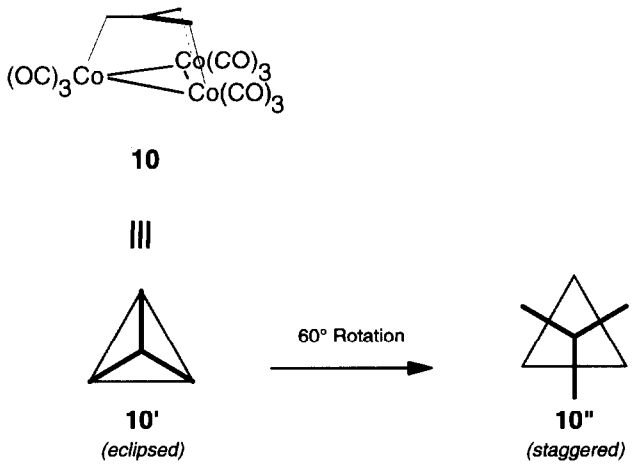

point of the W–Ni vector but instead closer to the tungsten center; this optimizes the antisymmetric component of the bonding. The symmetric component of the π-interaction of the TMM dianion with the nickel–tungsten fragment arises primarily via overlap of the metal HOMO with e_s. Since this involves two occupied orbitals, the overall effect is destabilizing and leads to a relatively high-lying HOMO in **3'**.

When the TMM ligand is aligned such that the allylic-type interaction is with the nickel atom, as in **3''**, the bonding interaction of e_a is markedly diminished, but this is partly compensated by the almost complete loss of the destabilizing overlap of the filled HOMO of the Ni–W fragment with the occupied e_s component of the TMM ligand. There is, however, a weaker two-orbital four-electron interaction of e_s with a mostly in-plane combination on the metallic moiety. The net result is an increased HOMO–LUMO gap for **3''** (0.81 eV) relative to that found in **3'** (0.62 eV), but total energy considerations favor the η^3-tungsten–η^1-nickel structure, which is found crystallographically for **3**.

In summary, although the TMM ligand is less firmly bonded to the dimetallic fragment in the W–Ni complex than it is in the Ru_2 case, there is a lower energy cost (34 kcal mol^{-1} for Ni–W *vs.* 42 kcal mol^{-1} for Ru_2) in going to the less favorable rotamer. In **2**, rotation through 30° brings about loss of the symmetrical component of the π-bonding between the TMM and the diruthenium unit; in the transformation of **3'** to **3''**, the diminished antisymmetric contribution to the bonding is partially counter-balanced by loss of the destabilizing symmetric interactions. Moreover, the hetero-bimetallic nature of **3** may be advantageous in that one can readily accommodate any unwanted charge by modifying the semi-bridging character of the carbonyls to siphon electron density to the other metal center. Interestingly, when the TMM ligand is rotated from **3'** to **3''** in 15° increments and the most favored

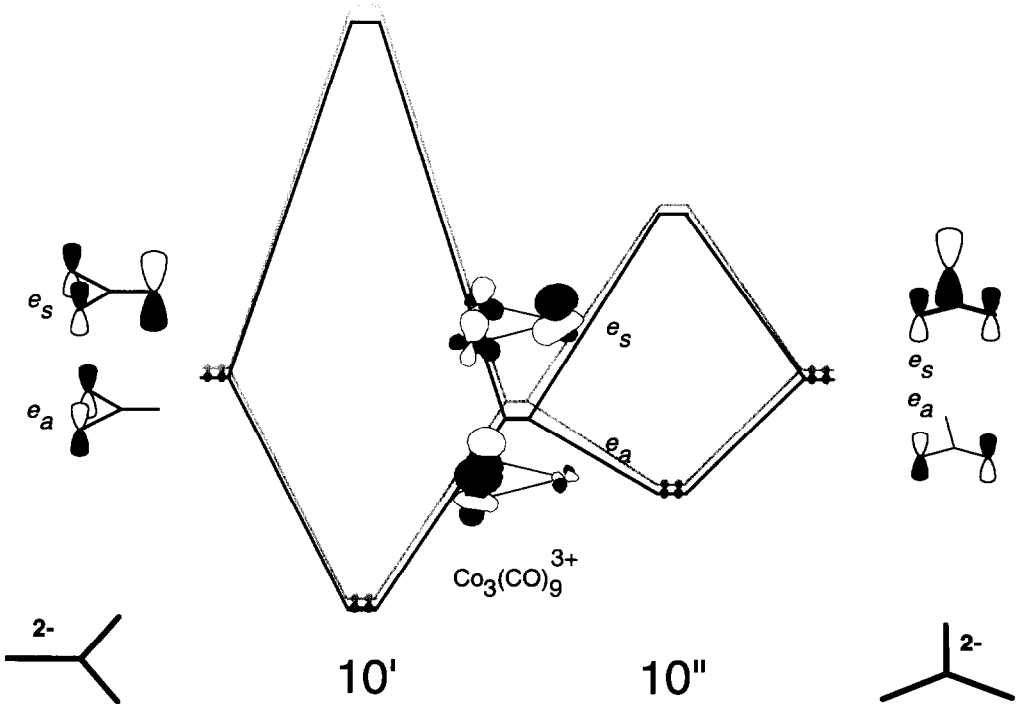

Fig. 5. Frontier orbital interaction diagram for the eclipsed, **10'**, and staggered, **10''**, rotamers of $[Co_3(CO)_9(TMM)]^+$.

structure calculated at each step, one must gradually decrease the interactions of the semi-bridging carbonyls with the nickel atom.

2.3. Trimetallic η^4-TMM complexes

The three-fold symmetry of TMM begs the question as to its possible stabilization by a trimetallic fragment. Thus, for instance, molecules are known in which an arene is coordinated in an η^2,η^2,η^2-fashion to a metal triangle [23]. We selected as our model the well-known fragment $[Co_3(CO)_9]^{3+}$, which has been extensively studied by Schilling and Hoffmann [24]. The calculations revealed that the cation $[(TMM)Co_3(CO)_9]^+$, **10**, should be a viable molecule in which the TMM ligand (which is optimally situated 2.2 Å above the cobalt triangle) prefers a planar geometry rather than the pyramidal structure found in the mono- and bi-metallic complexes **1**, **2** and **3**. The planar structure is required to allow the p orbitals on the three methylene arms to overlap satisfactorily with the vacant d_{z^2} orbitals on the cobalt vertices. Figure 5 shows how the doubly degenerate frontier orbitals of the $[TMM]^{2-}$ donor and $[Co_3(CO)_9]^{3+}$ acceptor sets yield a perfectly respectable HOMO–LUMO gap (1.62 eV). However, rotation of the TMM ligand from the eclipsed isomer, **10'**, to the staggered conformation, **10''**, not only halves the HOMO–LUMO gap but is also energetically disfavored to the tune of 34.6 $kcal^{-1}$. One could imagine that migration of a methylene group from one metal to another might involve a transition state in which the methylene rotates through 90° so as to maintain overlap with both metals. Such is certainly the case for methylene migrations in the tetrahedral cations such as $[Co_2(CO)_6(HC{\equiv}C\text{-}CH_2)]^+$ [25]. However, in **10**, orienting the planes of the CH_2 groups parallel to the three-fold axis of the cation is greatly disfavored. We conclude that the tricobalt–TMM cation would adopt the eclipsed conformation and would be non-fluxional.

Although we are unaware of any reports of any molecules analogous to **10**, one could readily visualize the synthesis of the isoelectronic neutral analogues $[(TMM)FeCo_2(CO)_9]$ or $[(TMM)FeMo_2(CO)_7Cp_2]$, perhaps by treatment of $(\eta^4\text{-TMM})Fe(CO)_3$ with a metal–metal triple-bonded precursor such as $Cp(CO)_2Mo{\equiv}Mo(CO)_2Cp$. Experiments are in progress to test this hypothesis.

3. Conclusions

In summary, it has been shown that the barrier to rotation of a TMM ligand relative to a mono-, di- or tri-metallic fragment is controlled primarily by the interactions of the e_s and e_a donor orbitals of the $[TMM]^{2-}$ with the frontier orbitals of the metal moieties. These examples serve to illustrate not merely how molecular orbital calculations can aid the synthetic or mechanistic organometallic chemist, but also that the user-friendly programs now available enable us to visualize the frontier orbitals of common organometallic fragments. Moreover, the facility with which one can calculate and plot hypersurfaces (such as Fig. 1) makes these useful in avoiding problems related to local minima.

4. Computational details

Molecular orbital calculations were performed within the extended Hückel formalism using weighted H_{ij}s [26–28]. Atomic parameters were taken from ref 17. Calculations were carried out by use of the program CACAO [29] on an EVERDATA 486–50 MHz IBM clone which required ≈ 90 min to generate the data from which the surface shown in Fig. 1 was constructed. EXCEL 4.0's "Chart Wizard" was used to generate the 3D surface as a mesh plot. Structural data were taken from refs. 1, 6 and 7. Molecules **3'** and **3''** were idealized versions of **3** in which the pentamethylcyclopentadienyl unit was replaced by a C_5H_5 ring.

Acknowledgements

Financial support from the Natural Sciences and Engineering Research Council of Canada is gratefully acknowledged. L.G. thanks Queen's University for internal scholarships.

References

1 A. Almenningen, A. Haaland and K. Wahl, *Acta Chem. Scand., 23* (1969) 1145.
2 T.A. Albright, P. Hofmann and R. Hoffmann, *J. Am. Chem. Soc., 99* (1977) 7546.
3 T.A. Albright, *Acc. Chem. Res., 15* (1982) 149.
4 L. Girard, J.H. MacNeil, A. Mansour, A.C. Chiverton, J.A. Page, S. Fortier and M.C. Baird, *Organometallics, 10* (1991) 3114.
5 L. Girard and M.C. Baird, *J. Organomet. Chem., 444* (1993) 143.
6 M.J. Fildes, S.A.R. Knox, A.G. Orpen, M.L. Orpen and M.I. Yates, *J. Chem. Soc., Chem. Commun.,* (1989) 1680.
7 M.J. Chetcuti, P.E. Fanwick and B.E. Grant, *Organometallics, 10* (1991) 3003.
8 E.S. Magyar and C.P. Lillya, *J. Organomet. Chem., 116* (1976) 99.
9 D.C. Andrews, G. Davidson and D.A. Duce, *J. Organomet. Chem., 97* (1975) 95.
10 D.H. Finseth, C. Sourisseau and F.A. Miller, *J. Phys. Chem., 80* (1976) 1248.
11 A.J. Rest, J.R. Sodeau and D.J. Taylor, *J. Chem. Soc., Dalton Trans.,* (1978) 651.
12 R.J. Clark, M.R. Abraham and M.A. Busch, *J. Organomet. Chem., 35* (1972) C33.
13 J.-M. Grosselin, H. Le Bozec, C. Moinet, L. Toupet, F.H. Kohler and P.H. Dixneuf, *Organometallics, 7* (1988) 88.
14 L. Girard and M.C. Baird, unpublished results.
15 B.M. Trost, *Angew. Chem. Int. Ed. Engl., 25* (1986) 1.

16 H. Vahrenkamp and D. Walter, *Organometallics, 1* (1982) 874.
17 J.-F. Halet, R. Hoffmann and J.-Y. Saillard, *Inorg. Chem., 24* (1985) 1695.
18 (a) H. Kwart and K. King, *d Orbitals in the Chemistry of Silicon, Phosphorus and Sulfur*, Springer, New York, 1977; (b) E.W. Abel, D.A. Armitage and D.B. Brady, *Trans. Farad. Soc., 62* (1966) 3459.
19 (a) S. Shambayati, J.F. Blake, S.G. Wierschke, W.L. Jorgensen and S.L. Schreiber, *J. Am. Chem. Soc., 112* (1990) 697; (b) J.A. Tossell, J.H. Moore, K. McMillan and M.A. Coplan, *J. Am. Chem. Soc., 113* (1991) 1031; (c) S. Xiao, W.C. Trogler, D.E. Ellis and Z. Berkovich-Yellin, *J. Am. Chem. Soc., 105* (1983) 7033 (d); D.S. Marynick, *J. Am. Chem. Soc., 106* (1984) 4064; (e) A.G. Orpen and N.G. Connelly, *Organometallics, 9* (1990) 1206; (f) B.J. Dunne, R.B. Morris and A.G. Orpen, *J. Chem. Soc., Dalton Trans.*, (1991) 6531.
20 PCMODEL, available from Serena Software, Box 3076, Bloomington, IN 47402-3076, USA.
21 J.J. Gajewski, K.E. Gilbert and J. McKelvey, *Adv. Molecular Modelling, 2* (1990) 65.
22 J.A.S. Howell, G. Walton, M.-C. Tirvengadum, A.D. Squibb, M.G. Palin, P. McArdle, D. Cunningham, Z. Goldschmidt, H. Gottlieb and G. Strul, *J. Organomet. Chem., 401* (1991) 91.
23 D. Braga, F. Grepioni, B.F.G. Johnson, J. Lewis, C.E. Housecroft and M. Martinelli, *Organometallics, 10* (1991) 1260, and references therein.
24 B.E.R. Schilling and R. Hoffmann, *J. Am. Chem. Soc., 101* (1979) 3456.
25 L. Girard, P.E. Lock, H. El Amouri and M.J. McGlinchey, *J. Organomet. Chem.*, (1994).
26 R. Hoffmann, *J. Chem. Phys., 39* (1963) 1397.
27 R. Hoffmann and W.N. Lipscomb, *J. Chem. Phys., 36* (1962) 2179; 3489.
28 J.H. Ammeter, H.B. Bürgi, J.C. Thibeault and R. Hoffmann, *J. Am. Chem. Soc., 100* (1978) 3686.
29 C. Mealli and D.M. Proserpio, *J. Chem. Ed., 67* (1990) 3399.